Signatures of hidden octupolar order from nonlinear Hall effects

Sopheak Sorn [1,*,†] and Adarsh S. Patri [2,*,‡]
[1] *Institute of Quantum Materials and Technology, Karlsruhe Institute of Technology, 76131 Karlsruhe, Germany*
[2] *Department of Physics, Massachusetts Institute of Technology, Cambridge, Massachusetts 02139, USA*

Detecting symmetry-breaking hidden orders with conventional probes has been a long-standing challenge in the field of magnetism. Higher-rank multipolar ordering—anisotropic charge and magnetization distributions arising from a combination of spin-orbit coupling and crystalline environments—is a quintessential example of such hidden orders, where new protocols of direct detection remain highly desirable. In this paper, we propose nonlinear Hall effects as a probe for multipolar ordering in metallic systems. Taking inspiration from the family of Pr-based heavy-fermion compounds, $Pr(Ti,V)_2Al_{20}$, we formulate a minimal cubic-lattice model of conduction electrons coupled to a ferro-octupolar order parameter. The time-reversal-breaking order leads to a band structure that supports strong quadrupolar moments of Berry curvature (BC). Using a semiclassical Boltzmann formalism in conjunction with a symmetry analysis, we demonstrate that the BC quadrupoles produce a third harmonic generation of the Hall voltage [$V_H(3\omega)$] measurable in an AC Hall experiment. Properties of the Hall response such as its anisotropy, its dissipationlessness, and its dependence on the order parameter are also examined. Our paper encourages an alternative realm of investigation of multipolar ordering from nonlinear transport experiments.

A deep understanding of quantum phases of matter ultimately requires experimental probes of the low-energy degrees of freedom. The celebrated Hall effect is an archetypal example supporting this philosophy, from the remarkable insight it can provide of the underlying properties of a system, ranging from the electron-hole nature of the charge carriers to the topology of the electronic band structure [1–5]. At the core of the Hall effects is the role of the Berry curvature (BC) of the occupied electronic bands. Semiclassically, for a spin-orbit-coupled system featuring a spin-imbalanced occupation number associated with a net magnetization, BC acts as a spin-dependent, momentum-space magnetic field to transversely deflect the electrons, giving rise to a well-defined Hall response [6–8]. Occurring even in the absence of a magnetic field, this anomalous Hall effect (AHE) scales with the magnetization, and can shed light on the canonical, ferromagnetically ordered ground state. This brings forth the intriguing question of whether Hall effect (or its generalizations) is flexible enough to provide discriminating signatures of unconventional broken-symmetry phases of matter.

Recently, nonlinear Hall effects, where the transverse Hall voltage scales nonlinearly with the applied charge current, have gained significant attention [9–20]. Nonlinear Hall effect can be understood as a natural multipolar extension of the mathematical AHE framework, where instead of merely considering the Brillouin-zone integral of the BC, one considers BC dipoles, BC quadrupoles, and beyond [9,10,12,17,20]. Due to the higher-rank nature of these BC multipolar moments, the resulting nonlinear Hall effects can arise even without a net magnetization. Indeed, evidence of BC-dipole-driven nonlinear Hall effect has been seen in a variety of nonmagnetic compounds [11,17,21–23] and in noncentrosymmetric compensated antiferromagnets [24] Similarly, there has been evidence of BC-quadrupole-driven nonlinear Hall effects in altermagnets [25], an emerging family of unconventional compensated collinear antiferromagnets [26,27].

This lack of magnetization is reminiscent of a class of d and f electronic systems, where localized electronic wave functions support higher-rank multipolar moments [28–30]. These anisotropic charge and magnetization densities (characterized by quadrupolar, octupolar, and higher-rank degrees of freedom) have been examined in a variety of contexts from actinide oxides (such as NpO_2 [31]) to f-electron heavy fermion systems [32–40] [including a system we will focus on here, $Pr(Ti,V)_2Al_{20}$] to pyrochlore quantum spin ices [$Ce_2(Sn,Zr)_2O_7$ [41–45] and $Pr_2(Hf,Sn,Zr)_2O_7$ [46–52]] and to d-electron compounds including osmates and rhenates [53–68]. Indeed, the orderings of higher-rank moments are notoriously difficult to directly detect with conventional local probes of magnetism, and have been appropriately placed under the umbrella of "hidden orders" [69]. Despite recent proposals to employ lattice-based protocols to detect multipole-based phenomena (such as magnetostriction, ultrasound, and impurity-induced strains [70–75]), it is still highly desirable to devise new probes in order to shine light on these phases of matter. With the aforementioned promising successes of Hall measurements in systems lacking a net magnetization, we are primed to examine the detection of multipolar orders within the framework of *nonlinear* Hall effects.

*These authors contributed equally to this work.
†Contact author: sopheak.sorn@kit.edu
‡Contact author: apatri@mit.edu

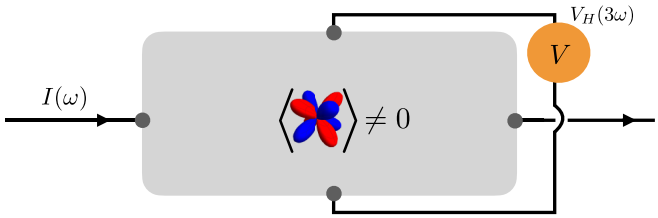

FIG. 1. Schematic of a Hall-bar configuration to realize the nonlinear Hall effect with an underlying octupolar order, $\phi \neq 0$. The third harmonic Hall response $\sigma^{(3\omega),H}_{abcd}$ is measured from the Hall voltage $V_H(3\omega)$ induced by an AC current $I(\omega)$ with a frequency ω.

In this paper, we explicitly demonstrate that metallic systems featuring a long-range ferro-octupolar order can be probed from a third-order Hall response. Taking a minimal cubic-lattice e_g electron model coupled to a ferro-octupolar order parameter, we show that the onset of the order opens gaps at various band crossing points and induces strong BC quadrupolar moments. The latter produces a third-harmonic generation detectable within a third-order Hall effect measurement (Fig. 1).

I. MINIMAL MODEL OF OCTUPOLAR ORDER

In the family of Pr-based rare-earth compounds, $Pr(Ti,V)_2Al_{20}$, the combination of strong spin-orbit coupling and crystal-electric-field effects leads the Pr^{3+} ions to host higher-rank multipolar moments: (1) time-reversal-even quadrupolar moments $O_{20} = \frac{1}{2}(3J_z^2 - J^2)$ and $O_{22} = \frac{\sqrt{3}}{2}(J_x^2 - J_y^2)$ and (2) a time-reversal-odd octupolar moment $\mathcal{T}_{xyz} = \frac{\sqrt{15}}{6}\overline{J_x J_y J_z}$; the overline indicates a symmetrized operator product over the angular-momentum Stevens operators. Via the conduction-electron-mediated Ruderman-Kittel-Kasuya-Yosida-like interaction between the localized moments, long-range ordering is permitted to develop. We consider the simple scenario of $\mathbf{q} = 0$ ferro-octupolar order given by the spatially uniform order parameter $\phi = \langle \mathcal{T}_{xyz} \rangle$.

Recent de Haas–van Alphen studies on $PrTi_2Al_{20}$ [76,77] have indicated a well-localized Fermi surface about the zone center. As such, the low-energy conduction electrons can be characterized in terms of irreducible representations of the corresponding O_h point group symmetry. In this paper, we consider the following Slater-Koster tight-binding model of e_g electrons on a cubic lattice, which is inspired by the Pr-based compounds:

$$\mathcal{H}_0(\mathbf{k}) = h_0(\mathbf{k})\tau^0 + h_1(\mathbf{k})\tau^x + h_3(\mathbf{k})\tau^z, \qquad (1)$$

where τ are Pauli matrices in the two-dimensional orbital space $\{d_{x^2-y^2}, d_{3z^2-r^2}\}$. $h_s(\mathbf{k})$ are the momentum-dependent form factors whose full expressions are given in the Supplemental Material (SM) [78]. Near the zone center, their quadratic-order expansions are given by simple expressions: $h_0(\mathbf{k}) = \text{const} + \tilde{\lambda}k^2$, $h_1(\mathbf{k}) = \frac{\sqrt{3}\lambda}{2}(k_x^2 - k_y^2)$, and $h_3(\mathbf{k}) = \frac{\lambda}{2}(3k_z^2 - k^2)$, where λ and $\tilde{\lambda}$ are associated with the overlap integrals (see SM).

Equipped with these orbital and spin degrees of freedom, the conduction electrons couple to the overlaying ferro-octupolar order via the symmetry-allowed term [79,80], $\mathcal{H}_\phi(\mathbf{k}) = \phi\tau^y$, where we have absorbed the coupling constant into the octupolar order parameter. We note that the spin plays the role of a spectator degree of freedom and is included as an implicit identity matrix in both the kinetic and coupling terms [79,80]. Therefore, the full model is $\mathcal{H}_0 + \mathcal{H}_\phi = h_0(\mathbf{k})\tau^0 + \mathbf{h}(\mathbf{k}) \cdot \boldsymbol{\tau}$, where $\mathbf{h} = (h_1, h_2, h_3)^T$. The band eigenvalues are $\varepsilon_{\mathbf{k},\pm} = h_0(\mathbf{k}) \pm |\mathbf{h}(\mathbf{k})|$.

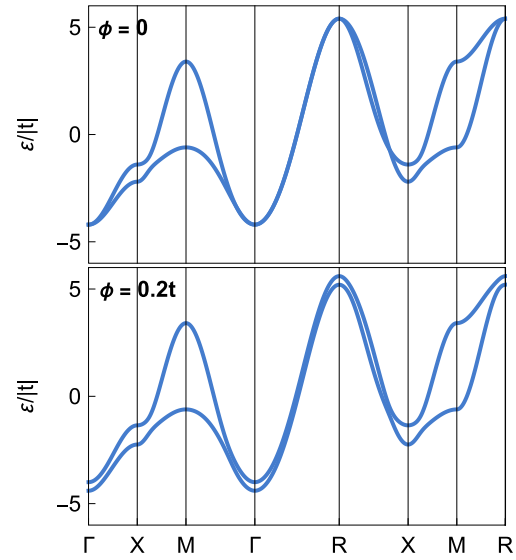

FIG. 2. Cubic-lattice electronic band structure in the absence (presence) of octupolar ordering ϕ. The octupolar ordering introduces a splitting of the degenerate band structure. The following overlap integrals, defined in SM [78], are used here and for the numerical results: $(t, u, v, w) = (-1, -0.6, -0.1, 0.2)$.

Figure 2 shows representative band structures in the absence and presence of the octupolar ordering. Notably when $\phi = 0$, there are many degenerate points such as those on the ΓM line and RX line. These degenerate points are protected by the mirror symmetry of the mirror planes: (110), (101), (011), $(\bar{1}10)$, $(\bar{1}01)$, and $(0\bar{1}1)$. On the other hand, the entire degenerate ΓR line is protected by the mirrors *and* the threefold rotation around the [111] axis; see SM [78] for a detailed description. A nonzero ϕ breaks these symmetries and lifts the degeneracy of the bands, leading to substantial BC near the gaps.

II. LINEAR AND NONLINEAR HALL EFFECTS

When $\phi \neq 0$, the magnetic point group of the system is $m\bar{3}m'$. Correspondingly, the linear response conductivity tensor σ_{ab} is proportional to a 3×3 identity matrix in the Cartesian basis directions. The twofold rotational symmetries about the three coordinate axes set the off-diagonal elements to zero, while the diagonal elements are identical due to the threefold rotation around the [111] axis. Therefore, from these symmetry considerations, the anomalous Hall effect is absent; from linear response theory, one can see this explicitly from the vanishing Brillouin-zone integral of the BC, $\sum_n \int d\mathbf{k} f_0(\varepsilon_{\mathbf{k}n})\Omega_c^n(\mathbf{k}) = 0$, where n is the band index, and the local BC is $\boldsymbol{\Omega}^n(\mathbf{k}) = \nabla_{\mathbf{k}} \times i \langle \mathbf{k}n | \nabla_{\mathbf{k}} | \mathbf{k}n \rangle$. A similar analysis

(as described in SM [78]) shows that the the second-order Hall response is also zero due to the inversion symmetry.

The Hall physics of our system is thus dominated by the third-order response, where a third-order current, $j_a^{(3)}(t) = \mathrm{Re}[j_a^{(3)}(\omega)e^{i\omega t}]$, is induced by an applied electric field $E_a(t) = \mathrm{Re}[E_a(\omega)e^{i\omega t}]$. With a Hall-bar-like experimental setup in mind (Fig. 1), we restrict ourselves to the linearly polarized electric field, where $E_a(\omega)$ can be made real valued by redefining the initial time. The induced current can be expressed in terms of a third-order response function, $j_a^{(3)}(2\omega \pm \omega) = \sigma_{abcd}^{(2\omega\pm\omega)} E_b(\omega)E_c(\omega)E_d(\pm\omega)$. There are two types of currents with frequencies ω and 3ω. The rest of the paper will focus on the third-harmonic $\sigma_{abcd} \equiv \sigma_{abcd}^{(3\omega)}$, while a straightforward generalization to $\sigma_{abcd}^{(\omega)}$ is discussed in SM [78]. Using a semiclassical Boltzmann formalism, it can be shown that σ_{abcd} consists of two parts: $\sigma_{abcd} = \sigma_{abcd}^D + \sigma_{abcd}^H$, where σ_{abcd}^D is the time-reversal-even Drude-like part, and σ_{abcd}^H is the time-reversal-odd Hall-like part [9,10,12,20]:

$$\sigma_{abcd}^D = \frac{e^4}{4\hbar}\sum_n \int d\mathbf{k} \frac{f_0(\varepsilon_{\mathbf{k}n})\partial_a\partial_b\partial_c\partial_d\varepsilon_{\mathbf{k}n}}{(\widetilde{\hbar\omega})(\widetilde{\hbar 2\omega})(\widetilde{\hbar 3\omega})}, \tag{2}$$

$$\sigma_{abcd}^H = -\frac{e^4}{12\hbar}\frac{\epsilon_{hab}Q_{cdh} + \epsilon_{hac}Q_{dbh} + \epsilon_{had}Q_{bch}}{(\widetilde{\hbar\omega})(\widetilde{\hbar 2\omega})}, \tag{3}$$

where $\widetilde{m\omega} \equiv im\omega + 1/\tau$, m is an integer, and τ is the relaxation time in the Boltzmann formalism. Q_{abc}^n is the BC quadrupolar moment for a given band, which is manifestly odd under time reversal:

$$Q_{abc} \equiv \sum_n Q_{abc}^n = \sum_n \int d\mathbf{k} f_0(\varepsilon_{\mathbf{k}n})\partial_{k_a}\partial_{k_b}\Omega_c^n(\mathbf{k}). \tag{4}$$

Similarly, the induced current can be split into a Drude-like and a Hall-like part. The Levi-Civita symbol in Eq. (3) leads to an orthogonality between the Hall current and the applied field, so the Joule heating is absent. The rest of the paper will focus on the time-reversal-odd dissipationless response. We note that we have ignored a third-order nonlinear Hall contribution from a correction to the Berry connection due to the electric field since it is time-reversal even and can exist even without the octupolar order [14,81,82]; see SM [78] for further discussions.

The $m\bar{3}m'$ magnetic point group ensures that there is only one independent component of σ_{abcd}^H whose value is denoted by σ_H:

$$\begin{aligned}\sigma_{xxyy}^H = \sigma_{yyzz}^H = \sigma_{zzxx}^H = \sigma_H,\\ \sigma_{xxzz}^H = \sigma_{zzyy}^H = \sigma_{yyzz}^H = -\sigma_H,\end{aligned} \tag{5}$$

where $\sigma_H \propto Q_{xyz}$. For brevity, the components obtained from permuting the last three indices are not shown, while the rest of the σ_{abcd}^H components are zero.

III. ANISOTROPIC NATURE OF THE INDUCED HALL CURRENT

Using a spherical-coordinate representation of $\mathbf{E}(\omega) = |\mathbf{E}(\omega)|\hat{E}$, where $\hat{E} = (\cos\varphi\sin\theta, \sin\varphi\sin\theta, \cos\theta)^T$, the induced Hall current is given by

$$\mathbf{j}^H \sim \begin{pmatrix}\sin\theta\cos\varphi(\sin^2\theta\sin^2\varphi - \cos^2\theta)\\ \sin\theta\sin\varphi(\cos^2\theta - \sin^2\theta\cos^2\varphi)\\ \cos\theta\sin^2\varphi(\cos^2\varphi - \sin^2\varphi)\end{pmatrix}. \tag{6}$$

If we define $\hat{E}$ by a point on an S^2 sphere, $\mathbf{j}^H$ can be represented by a tangent vector at that point. In this manner, Fig. 3 illustrates the profile of $\mathbf{j}^H$ (blue arrows) featuring a strong dependence on the orientation of $\hat{E}$. The magnitude of $\mathbf{j}^H$ is given by the color map of the inner sphere. $\mathbf{j}^H$ vanishes at 14 points where $\hat{E}$ lies on the high-symmetry axes of [100], [010], [001], [111], [$\bar{1}$11], [1$\bar{1}$1], and [11$\bar{1}$].

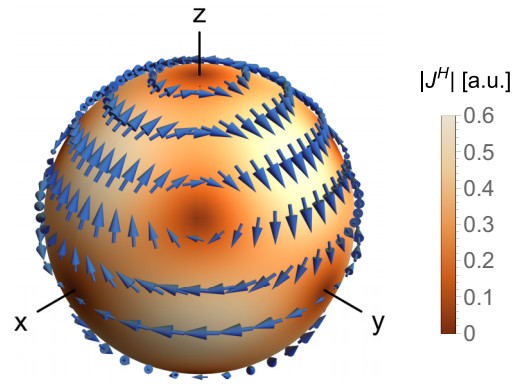

FIG. 3. Schematic illustration of the anisotropic nature of the nonlinear Hall response: at each point on S^2, the arrow lying in the tangent plane represents the induced Hall current $\mathbf{j}^H$ in response to an applied electric field (that is normal to the surface). The color map (and the size of the arrows) illustrates the magnitude of $\mathbf{j}^H$, which vanishes at 14 high-symmetry points.

IV. BERRY CURVATURE QUADRUPOLE

The magnitude of the Hall response is proportional to the BC quadrupole moments. In our model, BC is given by

$$\Omega_a^{\pm}(\mathbf{k}) = \mp\frac{\epsilon_{abc}}{4}\hat{h}\cdot\partial_{k_b}\hat{h}\times\partial_{k_c}\hat{h}, \tag{7}$$

where $\hat{h}(\mathbf{k}) = \mathbf{h}(\mathbf{k})/|\mathbf{h}(\mathbf{k})|$. $\Omega_a^{\pm}(\mathbf{k})$ is nonzero only when the vector field $\hat{h}(\mathbf{k})$ is locally noncoplanar. In the absence of the octupolar order, $\hat{h}(\mathbf{k})$ is coplanar, so BC vanishes everywhere. To provide intuition for this argument, it is instructive to consider the low-density limit, where the BC for the $\pm$ bands near the zone center is given by

$$\mathbf{\Omega}^{\pm}(\mathbf{k}) = \pm\frac{\sqrt{3}\lambda^2\phi}{\left(h_1^2 + h_3^2 + \phi^2\right)^{3/2}}(k_yk_z, k_xk_z, k_xk_y)^T. \tag{8}$$

We can clearly see that in the absence of the time-reversal-breaking octupolar order, BC vanishes as expected (as inversion is a symmetry in this cubic system). The corresponding BC quadrupole is given by

$$Q_{xyz}^{\pm} = \pm\sqrt{3}\lambda^2\int d\mathbf{k}\frac{F_1(\mathbf{k})\phi + F_3(\mathbf{k})\phi^3 - \phi^5}{\left(h_1^2 + h_3^2 + \phi^2\right)^{7/2}}. \tag{9}$$

$F_{1,3}$ are polynomial functions of momenta (see SM [78]).

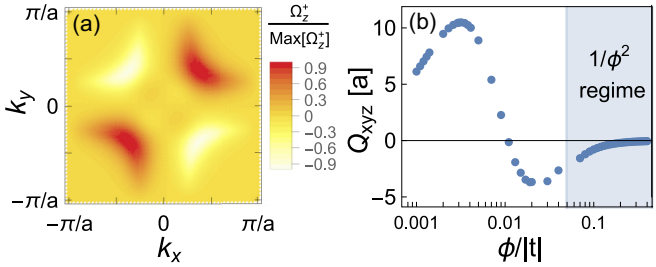

FIG. 4. (a) Reciprocal-space distribution of the Berry curvature, $\Omega_z^+(\mathbf{k})$, in the plane of $k_z = 0$, featuring a quadrupolar structure, which leads to a nontrivial Berry curvature quadrupole Q_{xyz} and a nonzero third-order Hall response. (b) Nonmonotonic dependence of Q_{xyz} on the octupolar order parameter ϕ. Q_{xyz} is expressed in the unit of the cubic-lattice constant, a. Note that the x axis is in a logarithmic scale. In the large-$|\phi|$ regime, Q_{xyz} scales as $1/\phi^2$, as explained in the main text.

Figure 4(a) shows the reciprocal-space profile of $\Omega_z^+(\mathbf{k}) = -\Omega_z^-(\mathbf{k})$ when $\phi/|t| = 0.2$ within the plane of $k_z = 0$. The BC profile possesses an azimuthal-angle dependence that is quadrupolar in nature, thus hinting at the BC quadrupole, Q_{xyz}. It is also apparent that there are BC hot spots with large BC concentration occurring near the gapped-out band crossing points along the ΓM line (as well as ΓR and RX lines) due to the octupolar order.

Figure 4(b) shows the dependence of Q_{xyz} on ϕ at a fixed, low electron density of $0.004/a^3$. As will be clear, the low density is chosen since it permits a partly tractable analysis of the ϕ dependence of Q_{xyz}; for numerical results at other densities, see SM [78]. Our main observation is that the strength of the third-order Hall response is a nonmonotonic function of the order parameter ϕ. This is rather unusual compared with, for instance, the linear Hall response of a ferromagnet, where it generally increases with the magnetization order parameter.[1]

To provide intuition it is once again instructive to return to the low-density limit. In the regime where $|\phi| \gg |t|$, we have two well-separated bands, and the electrons only occupy the lower band. Appealing to Eqs. (8) and (9), where the BC reduces to $\Omega_z^-(\mathbf{k}) = \frac{-\sqrt{3}\lambda^2 \mathrm{sgn}(\phi)}{\phi^2} k_x k_y$, we find that the BC quadrupole reduces to $Q_{xyz} \sim \frac{\mathrm{sgn}(\phi)}{\phi^2}$. This is in agreement with our numerical finding in Fig. 4(b). This regime ends when the upper band also becomes occupied as $|\phi|$ is lowered. It can be shown that, after and near the Lifshitz transition, the function $Q_{xyz}(\phi)$ no longer scales like $1/\phi^2$ and becomes more complicated, as also evident from the numerical results (see SM [78] for a discussion).

[1]Deviations can arise when there are additional features in the systems, e.g., Weyl points in the band structures, or an interplay between intrinsic and extrinsic AHE, or topological skyrmion spin textures. These can lead to a nonmonotonic relation between AHE and the magnetization. See, e.g., [3,83–87].

V. SIGNATURES IN THE AC HALL EXPERIMENT

A suitable way to measure the nonlinear Hall response due to the octupolar order is to perform a low-frequency[2] AC Hall experiment, where an AC current of a frequency ω is sent across a Hall bar, and the Hall voltage in the transverse direction at a frequency of 3ω is measured (see Fig. 1). To remove the Drude-like contribution from the third-order response, as in Eq. (3), the measured values need to be antisymmetrized between the two uniformly polarized domain measurements with the opposite order parameters, $\pm\phi$. A uniformly polarized octupolar domain could be procured, for example, by applying a magnetic field along the [111] direction [70]. The I-V relation between the amplitude of the applied current and that of the Hall voltage is expected to follow a cubic relation, $I \sim V^3$. Such a measurement is rather standard and has been used to measure various second-order Hall responses [17] and recently a third-order Hall response in FeSn [88]. For a future experimental design, it is worth emphasizing that the Hall response depends strongly on the orientation of the applied current relative to the crystallographic directions, as demonstrated by Fig. 3. Our results show that an appreciable BC quadrupole is possible in some parameter regime with $Q_{xyz} \approx 10^0$–10^2 Å [see Fig. 4(b) and assuming that the lattice constant $a \approx 14$ Å for $PrTi_2Al_{20}$ [89]]. Remarkably, this is of a comparable strength to that of the BC quadrupole in FeSn, where the third-order Hall effect has been measured [88].

VI. IMPACTS OF POSSIBLY COEXISTING MULTIPOLAR ORDERS

It is possible, yet not necessary, to have the octupolar order coexisting with other multipolar orders, e.g., the quadrupolar order, $\tilde{\phi} = \langle O_{22} \rangle$. $\tilde{\phi}$ alone does not break time-reversal symmetry, so the third-order Hall effect cannot be present with merely quadrupolar order. We have shown in SM [78] that, in the coexistence case starting with a nonzero ϕ, a growing $\tilde{\phi}$ increasingly suppresses BC quadrupoles. This outcome is attributed to the smearing effect of $\tilde{\phi}$ on the BC distribution. This can also be understood from the large-$\tilde{\phi}$ limit, as $\tilde{\phi}$ opens gaps at symmetry-protected band crossing points, but it does not produce any BC hot spots (see SM); a nonzero ϕ no longer generates BC hot spots like before, hence a smoother BC distribution and smaller BC quadrupoles. Therefore, the third-order Hall response is the largest when ϕ stands alone.

VII. DISCUSSION

In this paper, we demonstrated that a metallic system with ferro-octupolar order can exhibit a dissipationless third-order time-reversal-odd Hall response as a leading Hall phenomenon. This provides a means to detect the onset of octupolar order. We emphasized that this Hall effect arises despite the lack of a dipole moment, and we highlighted the key role of the Berry curvature quadrupole and its highly

[2]The low frequency is suited with the Boltzmann formalism since the interband transitions are suppressed; see [17] for a discussion.

nontrivial dependence on the octupolar order parameter. Our paper encourages experimental investigations of multipolar ordering using nonlinear Hall measurements (and more generally nonlinear transport studies [18,90]), in particular in the Pr-based systems. Future theoretical studies are required to incorporate the effects of impurities, order parameter fluctuations, as well as influence of Kondo-like effects [79,80,91,92] on nonlinear Hall response.

ACKNOWLEDGMENTS

We would like to thank Arun Paramekanti and Markus Garst for very helpful discussions. S.S. is supported by the Deutsche Forschungsgemeinschaft through TRR 288 Grant No. 422213477 (Project No. A11). A.S.P. is supported by a Simons Investigator Award from the Simons Foundation.

[1] D. J. Thouless, M. Kohmoto, M. P. Nightingale, and M. den Nijs, Quantized Hall conductance in a two-dimensional periodic potential, Phys. Rev. Lett. **49**, 405 (1982).

[2] K. von Klitzing, The quantized Hall effect, Rev. Mod. Phys. **58**, 519 (1986).

[3] N. Nagaosa, J. Sinova, S. Onoda, A. H. MacDonald, and N. P. Ong, Anomalous Hall effect, Rev. Mod. Phys. **82**, 1539 (2010).

[4] C.-X. Liu, S.-C. Zhang, and X.-L. Qi, The quantum anomalous Hall effect: Theory and experiment, Annu. Rev. Condens. Matter Phys. **7**, 301 (2016).

[5] J. Sinova, S. O. Valenzuela, J. Wunderlich, C. H. Back, and T. Jungwirth, Spin Hall effects, Rev. Mod. Phys. **87**, 1213 (2015).

[6] R. Karplus and J. M. Luttinger, Hall effect in ferromagnetics, Phys. Rev. **95**, 1154 (1954).

[7] M.-C. Chang and Q. Niu, Berry phase, hyperorbits, and the Hofstadter spectrum: Semiclassical dynamics in magnetic Bloch bands, Phys. Rev. B **53**, 7010 (1996).

[8] G. Sundaram and Q. Niu, Wave-packet dynamics in slowly perturbed crystals: Gradient corrections and Berry-phase effects, Phys. Rev. B **59**, 14915 (1999).

[9] I. Sodemann and L. Fu, Quantum nonlinear Hall effect induced by Berry curvature dipole in time-reversal invariant materials, Phys. Rev. Lett. **115**, 216806 (2015).

[10] T. Morimoto, S. Zhong, J. Orenstein, and J. E. Moore, Semiclassical theory of nonlinear magneto-optical responses with applications to topological Dirac/Weyl semimetals, Phys. Rev. B **94**, 245121 (2016).

[11] Q. Ma *et al.*, Observation of the nonlinear Hall effect under time-reversal-symmetric conditions, Nature (London) **565**, 337 (2019).

[12] Z.-F. Zhang, Z.-G. Zhu, and G. Su, Theory of nonlinear response for charge and spin currents, Phys. Rev. B **104**, 115140 (2021).

[13] Y. Gao and D. Xiao, Nonreciprocal directional dichroism induced by the quantum metric dipole, Phys. Rev. Lett. **122**, 227402 (2019).

[14] S. Lai, H. Liu, Z. Zhang, J. Zhao, X. Feng, N. Wang, C. Tang, Y. Liu, K. S. Novoselov, S. A. Yang, and W.-B. Gao, Third-order nonlinear Hall effect induced by the Berry-connection polarizability tensor, Nat. Nanotechnol. **16**, 869 (2021).

[15] C. Wang, Y. Gao, and D. Xiao, Intrinsic nonlinear Hall effect in antiferromagnetic tetragonal CuMnAs, Phys. Rev. Lett. **127**, 277201 (2021).

[16] H. Liu, J. Zhao, Y.-X. Huang, W. Wu, X.-L. Sheng, C. Xiao, and S. A. Yang, Intrinsic second-order anomalous Hall effect and its application in compensated antiferromagnets, Phys. Rev. Lett. **127**, 277202 (2021).

[17] Z. Z. Du, H.-Z. Lu, and X. C. Xie, Nonlinear Hall effects, Nat. Rev. Phys. **3**, 744 (2021).

[18] Y. Michishita and N. Nagaosa, Dissipation and geometry in nonlinear quantum transports of multiband electronic systems, Phys. Rev. B **106**, 125114 (2022).

[19] Y. Liu, H. Watanabe, and N. Nagaosa, Emergent magnetomultipoles and nonlinear responses of a magnetic hopfion, Phys. Rev. Lett. **129**, 267201 (2022).

[20] C.-P. Zhang, X.-J. Gao, Y.-M. Xie, H. C. Po, and K. T. Law, Higher-order nonlinear anomalous Hall effects induced by Berry curvature multipoles, Phys. Rev. B **107**, 115142 (2023).

[21] K. Kang, T. Li, E. Sohn, J. Shan, and K. F. Mak, Nonlinear anomalous Hall effect in few-layer WTe_2, Nat. Mater. **18**, 324 (2019).

[22] J.-X. Hu, C.-P. Zhang, Y.-M. Xie, and K. T. Law, Nonlinear Hall effects in strained twisted bilayer WSe_2, Commun. Phys. **5**, 255 (2022).

[23] M. Huang, Z. Wu, J. Hu, X. Cai, E. Li, L. An, X. Feng, Z. Ye, N. Lin, K. T. Law, and N. Wang, Giant nonlinear Hall effect in twisted bilayer WSe_2, Natl. Sci. Rev. **10**, nwac232 (2023).

[24] D.-F. Shao, S.-H. Zhang, G. Gurung, W. Yang, and E. Y. Tsymbal, Nonlinear anomalous Hall effect for Néel vector detection, Phys. Rev. Lett. **124**, 067203 (2020).

[25] Y. Fang, J. Cano, and S. A. A. Ghorashi, Quantum geometry induced nonlinear transport in altermagnets, Phys. Rev. Lett. **133**, 106701 (2024).

[26] L. Šmejkal, J. Sinova, and T. Jungwirth, Emerging research landscape of altermagnetism, Phys. Rev. X **12**, 040501 (2022).

[27] L. Šmejkal, J. Sinova, and T. Jungwirth, Beyond conventional ferromagnetism and antiferromagnetism: A phase with nonrelativistic spin and crystal rotation symmetry, Phys. Rev. X **12**, 031042 (2022).

[28] Y. Kuramoto, H. Kusunose, and A. Kiss, Multipole orders and fluctuations in strongly correlated electron systems, J. Phys. Soc. Jpn. **78**, 072001 (2009).

[29] H. Kusunose, Description of multipole in f-electron systems, J. Phys. Soc. Jpn. **77**, 064710 (2008).

[30] P. Santini, S. Carretta, G. Amoretti, R. Caciuffo, N. Magnani, and G. H. Lander, Multipolar interactions in f-electron systems: The paradigm of actinide dioxides, Rev. Mod. Phys. **81**, 807 (2009).

[31] Y. Tokunaga, D. Aoki, Y. Homma, S. Kambe, H. Sakai, S. Ikeda, T. Fujimoto, R. E. Walstedt, H. Yasuoka, E. Yamamoto, A. Nakamura, and Y. Shiokawa, NMR evidence for higher-order multipole order parameters in NpO_2, Phys. Rev. Lett. **97**, 257601 (2006).

[32] T. Onimaru and H. Kusunose, Exotic quadrupolar phenomena in non-Kramers doublet systems: The cases of PrT_2Zn_{20}

(T = Ir, Rh) and PrT_2Al_{20} (T = V, Ti), J. Phys. Soc. Jpn. **85**, 082002 (2016).
[33] M. Tsujimoto, Y. Matsumoto, T. Tomita, A. Sakai, and S. Nakatsuji, Heavy-fermion superconductivity in the quadrupole ordered state of PrV_2Al_{20}, Phys. Rev. Lett. **113**, 267001 (2014).
[34] L. Ye, M. E. Sorensen, M. D. Bachmann, and I. R. Fisher, Measurement of the magnetic octupole susceptibility of PrV_2Al_{20}, Nat Commun. **15**, 7005 (2024).
[35] P. Chandra, P. Coleman, J. A. Mydosh, and V. Tripathi, Hidden orbital order in the heavy fermion metal URu_2Si_2, Nature (London) **417**, 831 (2002).
[36] V. Tripathi, P. Chandra, and P. Coleman, Sleuthing hidden order, Nat. Phys. **3**, 78 (2007).
[37] A. F. Santander-Syro, M. Klein, F. L. Boariu, A. Nuber, P. Lejay, and F. Reinert, Fermi-surface instability at the "hidden-order" transition of URu_2Si_2, Nat. Phys. **5**, 637 (2009).
[38] K. Haule and G. Kotliar, Arrested Kondo effect and hidden order in URu_2Si_2, Nat. Phys. **5**, 796 (2009).
[39] R. Okazaki, T. Shibauchi, H. J. Shi, Y. Haga, T. D. Matsuda, E. Yamamoto, Y. Onuki, H. Ikeda, and Y. Matsuda, Rotational symmetry breaking in the hidden-order phase of URu_2Si_2, Science **331**, 439 (2011).
[40] J. G. Rau and H.-Y. Kee, Hidden and antiferromagnetic order as a rank-5 superspin in URu_2Si_2, Phys. Rev. B **85**, 245112 (2012).
[41] R. Sibille, E. Lhotel, V. Pomjakushin, C. Baines, T. Fennell, and M. Kenzelmann, Candidate quantum spin liquid in the Ce^{3+} pyrochlore stannate $Ce_2Sn_2O_7$, Phys. Rev. Lett. **115**, 097202 (2015).
[42] B. Gao *et al.*, Experimental signatures of a three-dimensional quantum spin liquid in effective spin-1/2 $Ce_2Zr_2O_7$ pyrochlore, Nat. Phys. **15**, 1052 (2019).
[43] J. Gaudet, E. M. Smith, J. Dudemaine, J. Beare, C. R. C. Buhariwalla, N. P. Butch, M. B. Stone, A. I. Kolesnikov, G. Xu, D. R. Yahne, K. A. Ross, C. A. Marjerrison, J. D. Garrett, G. M. Luke, A. D. Bianchi, and B. D. Gaulin, Quantum spin ice dynamics in the dipole-octupole pyrochlore magnet $Ce_2Zr_2O_7$, Phys. Rev. Lett. **122**, 187201 (2019).
[44] R. Sibille, N. Gauthier, E. Lhotel, V. Porée, V. Pomjakushin, R. A. Ewings, T. G. Perring, J. Ollivier, A. Wildes, C. Ritter, T. C. Hansen, D. A. Keen, G. J. Nilsen, L. Keller, S. Petit, and T. Fennell, A quantum liquid of magnetic octupoles on the pyrochlore lattice, Nat. Phys. **16**, 546 (2020).
[45] E. M. Smith *et al.*, Case for a $U(1)_\pi$ quantum spin liquid ground state in the dipole-octupole pyrochlore $Ce_2Zr_2O_7$, Phys. Rev. X **12**, 021015 (2022).
[46] R. Sibille, E. Lhotel, M. C. Hatnean, G. Balakrishnan, B. Fåk, N. Gauthier, T. Fennell, and M. Kenzelmann, Candidate quantum spin ice in the pyrochlore $Pr_2Hf_2O_7$, Phys. Rev. B **94**, 024436 (2016).
[47] V. K. Anand, L. Opherden, J. Xu, D. T. Adroja, A. T. M. N. Islam, T. Herrmannsdörfer, J. Hornung, R. Schönemann, M. Uhlarz, H. C. Walker, N. Casati, and B. Lake, Physical properties of the candidate quantum spin-ice system $Pr_2Hf_2O_7$, Phys. Rev. B **94**, 144415 (2016).
[48] R. Sibille, N. Gauthier, H. Yan, M. Ciomaga Hatnean, J. Ollivier, B. Winn, U. Filges, G. Balakrishnan, M. Kenzelmann, N. Shannon, and T. Fennell, Experimental signatures of emergent quantum electrodynamics in $Pr_2Hf_2O_7$, Nat. Phys. **14**, 711 (2018).
[49] P. M. Sarte, A. A. Aczel, G. Ehlers, C. Stock, B. D. Gaulin, C. Mauws, M. B. Stone, S. Calder, S. E. Nagler, J. W. Hollett, H. D. Zhou, J. S. Gardner, J. P. Attfield, and C. R. Wiebe, Evidence for the confinement of magnetic monopoles in quantum spin ice, J. Phys.: Condens. Matter **29**, 45LT01 (2017).
[50] A. J. Princep, D. Prabhakaran, A. T. Boothroyd, and D. T. Adroja, Crystal-field states of Pr^{3+} in the candidate quantum spin ice $Pr_2Sn_2O_7$, Phys. Rev. B **88**, 104421 (2013).
[51] H. D. Zhou, C. R. Wiebe, J. A. Janik, L. Balicas, Y. J. Yo, Y. Qiu, J. R. D. Copley, and J. S. Gardner, Dynamic spin ice: $Pr_2Sn_2O_7$, Phys. Rev. Lett. **101**, 227204 (2008).
[52] K. Kimura, S. Nakatsuji, J.-J. Wen, C. Broholm, M. B. Stone, E. Nishibori, and H. Sawa, Quantum fluctuations in spin-ice-like $Pr_2Zr_2O_7$, Nat. Commun. **4**, 1934 (2013).
[53] G. Chen, R. Pereira, and L. Balents, Exotic phases induced by strong spin-orbit coupling in ordered double perovskites, Phys. Rev. B **82**, 174440 (2010).
[54] G. Chen and L. Balents, Spin-orbit coupling in d^2 ordered double perovskites, Phys. Rev. B **84**, 094420 (2011).
[55] L. Fu, Parity-breaking phases of spin-orbit-coupled metals with gyrotropic, ferroelectric, and multipolar orders, Phys. Rev. Lett. **115**, 026401 (2015).
[56] J. W. Harter, Z. Y. Zhao, J.-Q. Yan, D. G. Mandrus, and D. Hsieh, A parity-breaking electronic nematic phase transition in the spin-orbit coupled metal $Cd_2Re_2O_7$, Science **356**, 295 (2017).
[57] L. Lu, M. Song, W. Liu, A. P. Reyes, P. Kuhns, H. O. Lee, I. R. Fisher, and V. F. Mitrović, Magnetism and local symmetry breaking in a Mott insulator with strong spin orbit interactions, Nat. Commun. **8**, 14407 (2017).
[58] S. Hayami, H. Kusunose, and Y. Motome, Emergent odd-parity multipoles and magnetoelectric effects on a diamond structure: Implication for the 5*d* transition metal oxides $AOsO_4$(a = K, Rb, and Cs), Phys. Rev. B **97**, 024414 (2018).
[59] D. Hirai and Z. Hiroi, Successive symmetry breaking in a Jeff = 3/2 quartet in the spin-orbit coupled insulator Ba_2MgReO_6, J. Phys. Soc. Jpn. **88**, 064712 (2019).
[60] D. D. Maharaj, G. Sala, M. B. Stone, E. Kermarrec, C. Ritter, F. Fauth, C. A. Marjerrison, J. E. Greedan, A. Paramekanti, and B. D. Gaulin, Octupolar versus Néel order in cubic $5d^2$ double perovskites, Phys. Rev. Lett. **124**, 087206 (2020).
[61] A. Paramekanti, D. D. Maharaj, and B. D. Gaulin, Octupolar order in *d*-orbital Mott insulators, Phys. Rev. B **101**, 054439 (2020).
[62] S. Voleti, D. D. Maharaj, B. D. Gaulin, G. Luke, and A. Paramekanti, Multipolar magnetism in *d*-orbital systems: Crystal field levels, octupolar order, and orbital loop currents, Phys. Rev. B **101**, 155118 (2020).
[63] S. W. Lovesey and D. D. Khalyavin, Lone octupole and bulk magnetism in osmate $5d^2$ double perovskites, Phys. Rev. B **102**, 064407 (2020).
[64] C. Svoboda, W. Zhang, M. Randeria, and N. Trivedi, Orbital order drives magnetic order in $5d^1$ and $5d^2$ double perovskite Mott insulators, Phys. Rev. B **104**, 024437 (2021).
[65] S. W. Lovesey, D. D. Khalyavin, G. van der Laan, and G. J. Nilsen, Diffraction by multipoles in a $5d^2$ rhenium double perovskite, Phys. Rev. B **103**, 104429 (2021).
[66] L. V. Pourovskii, D. F. Mosca, and C. Franchini, Ferro-octupolar order and low-energy excitations in d^2 double perovskites of osmium, Phys. Rev. Lett. **127**, 237201 (2021).

[67] G. Khaliullin, D. Churchill, P. P. Stavropoulos, and H.-Y. Kee, Exchange interactions, Jahn-Teller coupling, and multipole orders in pseudospin one-half $5d^2$ Mott insulators, Phys. Rev. Res. **3**, 033163 (2021).

[68] D. Churchill and H.-Y. Kee, Competing multipolar orders in a face-centered cubic lattice: Application to the osmium double perovskites, Phys. Rev. B **105**, 014438 (2022).

[69] J. A. Mydosh and P. M. Oppeneer, Colloquium: Hidden order, superconductivity, and magnetism: The unsolved case of URu_2Si_2, Rev. Mod. Phys. **83**, 1301 (2011).

[70] A. S. Patri, A. Sakai, S. Lee, A. Paramekanti, S. Nakatsuji, and Y. B. Kim, Unveiling hidden multipolar orders with magnetostriction, Nat. Commun. **10**, 4092 (2019).

[71] E. W. Rosenberg, J.-H. Chu, J. P. C. Ruff, A. T. Hristov, and I. R. Fisher, Divergence of the quadrupole-strain susceptibility of the electronic nematic system $YbRu_2Ge_2$, Proc. Natl. Acad. Sci. USA **116**, 7232 (2019).

[72] A. S. Patri, M. Hosoi, and Y. B. Kim, Distinguishing dipolar and octupolar quantum spin ices using contrasting magnetostriction signatures, Phys. Rev. Res. **2**, 023253 (2020).

[73] A. S. Patri, M. Hosoi, S. B. Lee, and Y. B. Kim, Theory of magnetostriction for multipolar quantum spin ice in pyrochlore materials, Phys. Rev. Res. **2**, 033015 (2020).

[74] S. Simon, A. S. Patri, and Y. B. Kim, Ultrasound detection of emergent photons in generic quantum spin ice, Phys. Rev. B **106**, 064427 (2022).

[75] S. Voleti, K. Pradhan, S. Bhattacharjee, T. Saha-Dasgupta, and A. Paramekanti, Probing octupolar hidden order via Janus impurities, npj Quantum Mater. **8**, 42 (2023).

[76] S. Nagashima, T. Nishiwaki, A. Otani, M. Sakoda, E. Matsuoka, H. Harima, and H. Sugawara, De Haas-van Alphen effect in RTi_2Al_{20} (R = La, Pr, and Sm), J. Phys. Soc. Jpn. Conf. Proc. **3**, 011019 (2014).

[77] T. Kubo, E. Matsuoka, H. Kotegawa, H. Tou, A. Nakamura, D. Aoki, H. Harima, and H. Sugawara, Fermi surface of the heavy-fermion superconductor $PrTi_2Al_{20}$, J. Phys. Soc. Jpn. **89**, 084704 (2020).

[78] See Supplemental Material at http://link.aps.org/supplemental/10.1103/PhysRevB.110.125127 for (1) more details on tight binding model, (2) symmetry protection of gapless points in the band structure, (3) complete non-linear Hall conductivity tensor and its properties, (4) vanishing of quadratic non-linear Hall response, (5) discussion on further Berry-curvature quadrupole contributions to nonlinear Hall effect, (6) numerical properties of the third-order Hall effect, (7) a discussion on the dependence of the third-order Hall effect on the octupolar order parameter, and (8) impacts of other possible coexisting order parameters on the Hall response.

[79] A. S. Patri, I. Khait, and Y. B. Kim, Emergent non-Fermi-liquid phenomena in multipolar quantum impurity systems, Phys. Rev. Res. **2**, 013257 (2020).

[80] A. S. Patri and Y. B. Kim, Critical theory of non-Fermi liquid fixed point in multipolar Kondo problem, Phys. Rev. X **10**, 041021 (2020).

[81] H. Liu, J. Zhao, Y.-X. Huang, X. Feng, C. Xiao, W. Wu, S. Lai, W.-B. Gao, and S. A. Yang, Berry connection polarizability tensor and third-order Hall effect, Phys. Rev. B **105**, 045118 (2022).

[82] X.-G. Ye, P.-F. Zhu, W.-Z. Xu, Z. Zang, Y. Ye, and Z.-M. Liao, Orbital polarization and third-order anomalous Hall effect in WTe_2, Phys. Rev. B **106**, 045414 (2022).

[83] N. Haham, Y. Shperber, M. Schultz, N. Naftalis, E. Shimshoni, J. W. Reiner, and L. Klein, Scaling of the anomalous Hall effect in $SrRuO_3$, Phys. Rev. B **84**, 174439 (2011).

[84] Y. Chen, D. L. Bergman, and A. A. Burkov, Weyl fermions and the anomalous Hall effect in metallic ferromagnets, Phys. Rev. B **88**, 125110 (2013).

[85] F. M. Bartram, S. Sorn, Z. Li, K. Hwangbo, S. Shen, F. Frontini, L. He, P. Yu, A. Paramekanti, and L. Yang, Anomalous Kerr effect in $SrRuO_3$ thin films, Phys. Rev. B **102**, 140408(R) (2020).

[86] M. Lee, W. Kang, Y. Onose, Y. Tokura, and N. P. Ong, Unusual Hall effect anomaly in MnSi under pressure, Phys. Rev. Lett. **102**, 186601 (2009).

[87] A. Neubauer, C. Pfleiderer, B. Binz, A. Rosch, R. Ritz, P. G. Niklowitz, and P. Böni, Topological Hall effect in the *a* phase of MnSi, Phys. Rev. Lett. **102**, 186602 (2009).

[88] S. Sankar, R. Liu, X.-J. Gao, Q.-F. Li, C. Chen, C.-P. Zhang, J. Zheng, Y.-H. Lin, K. Qian, R.-P. Yu *et al.*, Observation of the Berry curvature quadrupole induced nonlinear anomalous Hall effect at room temperature, arXiv:2303.03274.

[89] T. Taniguchi, M. Yoshida, H. Takeda, M. Takigawa, M. Tsujimoto, A. Sakai, Y. Matsumoto, and S. Nakatsuji, Single crystal 27Al-NMR study of the cubic γ_3 ground doublet system $PrTi_2Al_{20}$, J. Phys.: Conf. Ser. **683**, 012016 (2016).

[90] J. Ahn, G.-Y. Guo, and N. Nagaosa, Low-frequency divergence and quantum geometry of the bulk photovoltaic effect in topological semimetals, Phys. Rev. X **10**, 041041 (2020).

[91] G. Zhang, J. S. Van Dyke, and R. Flint, Cubic hastatic order in the two-channel Kondo-Heisenberg model, Phys. Rev. B **98**, 235143 (2018).

[92] D. J. Schultz, A. S. Patri, and Y. B. Kim, Rise and fall of non-Fermi liquid fixed points in multipolar Kondo problems, Phys. Rev. Res. **3**, 013189 (2021).